Inorganic Chemistry

Article

pubs.acs.org/IC

Hetero-multinuclear Ruthenium(III)/Platinum(II) Complexes That Potentially Exhibit Both Antimetastatic and Antineoplastic Properties

Craig M. Anderson,*[,†] Isabelle R. Taylor,[†] Michael F. Tibbetts,[‡] Jessica Philpott,[‡] Yongfeng Hu,[§] and Joseph M. Tanski[⊥]

[†]Department of Chemistry and [‡]Department of Biology, Bard College, 30 Campus Rd, Annandale-on-Hudson, New York 12504, United States

[§]Canadian Light Source, 101 Perimeter Road, Saskatoon, SK S7N 0X4, Canada

[⊥]Department of Chemistry, Vassar College, 124 Raymond Avenue, Box 601, Poughkeepsie, New York 12604, United States

Supporting Information

ABSTRACT: Hetero-multinuclear, platinum/ruthenium species were synthesized and tested for their effect on the motility of A549 (nonsmall cell lung) and MDA-MB-231 (breast) cancer cells and for their ability to inhibit DNA mobility using gel electrophoresis. It was found that the Ru_2Pt trinuclear species $[Na_2]\{[Ru^{III}Cl_4(DMSO\text{-}S)(\text{-}\mu\text{-}pyz)]_2Pt^{II}Cl_2\}$, AH197, was much more efficient at inhibiting cell motility than $[C_3N_2H_5][Ru^{III}Cl_4(DMSO\text{-}S)(C_3N_2H_4)]$, NAMI-A, while the dinuclear RuPt species $[K][Ru^{III}Cl_4(DMSO\text{-}S)(\text{-}\mu\text{-}pyz)\text{-}Pt^{II}(DMSO\text{-}S)Cl_2]$, IT127, was slightly better than NAMI-A. However, the dinuclear species retarded the electrophoretic mobility of DNA greater than both the trinuclear complex and cisplatin. The metal complexes and their respective BSA protein/metal adducts were studied by X-ray absorption spectroscopy. The spectra led to the conclusion that BSA donor atoms have substituted for the chloride ligands and perhaps the DMSO ligands.

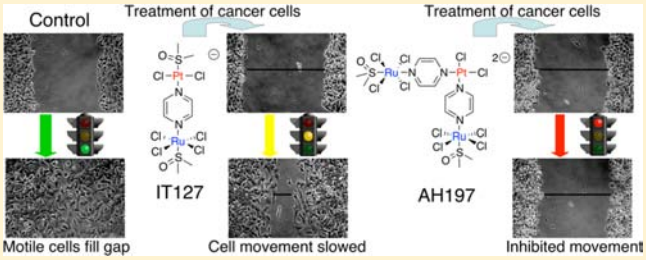

INTRODUCTION

Cancer is a disease for which a wide variety of treatments have been implemented over the years, including chemotherapy, radiation, and the surgical removal of tumors.[1] The use of platinum complexes as chemotherapeutic agents is a practice that has reigned in the treatment of the disease since the platinum-based drug, cisplatin, was introduced almost four decades ago.[2] Unfortunately, while many forms of chemotherapy, including treatment with cisplatin, can be extraordinarily effective in treating primary cancers, many of these drugs fail to remain effective once the cancer has become malignant.[3] For this reason, along with adverse side effects and drug resistance associated with cisplatin and other platinum-based drugs, new pharmaceutical agents featuring alternative metals have been sought out.[4]

In more recent years, ruthenium complexes have shown promise both as antiproliferative and as antimetastatic agents with a few of these compounds currently in clinical trials.[5] NAMI-A, a well-studied ruthenium(III) species, has been shown to bind to serum proteins and both the drug and drug/protein adduct have been shown to significantly inhibit cancer cell motility, possibly accounting for its general antimetastatic activity.[6] The antimetastatic nature of NAMI-A is particularly promising in that it could potentially pick up where other, more traditional drugs leave off, in treating the later stages of malignant cancers.

It has been suggested that multinuclear complexes with different metal centers (hetero-multinuclear) could potentially exhibit a synergistic effect, thus having a greater impact on their target biological system than the individual complexes separately. For example, many multinuclear platinum species have been reported to have unique behaviors and exhibit different interactions with DNA in comparison to cisplatin.[7] In addition, hetero-multinuclear platinum/ruthenium complexes have been reported to show interesting photoinduced DNA modification and cleavage.[8] Recently, we have reported multinuclear species, including the trinuclear species, AH197, $[Na_2]\{[Ru^{III}Cl_4(DMSO\text{-}S)(\text{-}\mu\text{-}pyz)]_2Pt^{II}Cl_2\}$ that has both ruthenium(III) and platinum(II) fragments with the hope of incorporating the best properties of both classes of drugs.[9] AH197 was shown to interact with DNA in a greater fashion than cisplatin.[9a]

Due to the inherent difficulty in characterizing ruthenium(III) complexes by routine NMR spectra, as a result of the presence of a paramagnetic nucleus, alternative spectroscopic methods must be employed in order to study the progress of their reactions or identify intermediates and final products.[10] A few examples of alternative methods that have been explored recently in the characterization of ruthenium(III) complexes

Received: September 11, 2012
Published: November 14, 2012

and their interaction with biomolecules include electron paramagnetic resonance (EPR), UV/visible, and X-ray absorption spectroscopy (XAS). EPR has very recently been used successfully as a limited spectroscopic tool to monitor the reduction of ruthenium(III) to ruthenium(II), in NAMI-type complexes, as an "off/on" detector, where the EPR signal is silent for diamagnetic ruthenium(II).[11] This aids in the characterization of active species in vivo, as ruthenium(III) complexes are speculated to act as prodrugs with an "activation by reduction" mechanism.[2a] XAS is a valuable technique that has been employed recently that can give information about the oxidation state of the metal and the nature of the coordinated ligands, and hence about the substitution processes occurring at the metal.[12] UV/vis spectroscopy is a very accessible but limited technique that can also be used to monitor a reaction. It has been used to monitor the progress of reactions between ruthenium complexes and BSA.[13] In this article, we report the synthesis and reactivity of hetero-multinuclear species featuring paramagnetic ruthenium(III) centers as well as classic platinum(II) centers. These include the previously reported trinuclear Ru_2Pt species (AH197), as well as a new dinuclear RuPt species (IT127). In order to assess the potential of these complexes as antimetastatic and/or antineoplastic agents, they were tested for their effect on motility in two cancer cell lines and on DNA electrophoretic mobility. Additionally, we have used XAS and UV/vis spectroscopies to evaluate the reactions of the metal complexes with the serum protein, bovine serum albumin (BSA).

EXPERIMENTAL SECTION

General. ^{1}H- and ^{13}C-NMR spectra were recorded using a Varian 400 MHz (^{1}H, 400 MHz; ^{13}C, 100 MHz) spectrometer and referenced to $SiMe_4$ (^{1}H, ^{13}C). δ values are given in parts per million, and J values are in hertz. IR spectra were recorded on a Thermo-Nicolet FT-IR Spectrophotometer with a diamond ATR. UV−vis spectra were recorded using Agilent 8453 and Varian Cary 100 spectrophotometers. Elemental analyses were done by Robertson Microlit Laboratories Inc., Ledgewood, New Jersey. Na[*trans*-$RuCl_4$(DMSO)(pyz)] (AH403), K[$PtCl_3$(DMSO-S)], and NAMI-A were synthesized according to reported procedures (Chart 1)[14] (pyz = pyrazine).

[K][$Ru^{III}Cl_4$(DMSO-S)(-μ-pyz)Pt^{II}(DMSO-S)Cl_2] (IT127). A 0.10 g portion of Na[*trans*-$RuCl_4$(DMSO)(pyz)] (0.24 mmol) was dissolved in 2 mL water and added to a stirring solution of 0.10 g K[$PtCl_3$(DMSO-S)] (0.24 mmol), also dissolved in 2 mL water. The solution was stirred at room temperature for 1 h, after which ethanol (200 proof) was added in excess to the solution and left at 4 °C overnight. A red-orange powder was collected, washed with diethyl ether, and vacuum-dried. A 0.09 g portion was obtained (48%). The complex was formulated as having the potassium cation, as determined by atomic emission spectroscopy.[15] A 7.0 mg solution of IT127 in 10.0 mL was determined to be 32(3) ppm in K^+ and 2(1) ppm in Na^+. Calculated K^+ parts per million for $C_{10}H_{22}Cl_6KN_2O_3PtRuS_2$ (IT127·CH_3CH_2OH): 33 ppm. Elemental analysis: Calculated percent for $C_{10}H_{22}Cl_6KN_2O_3PtRuS_2$ (IT127·CH_3CH_2OH): C, 14.46; H, 2.67; N, 3.37; Cl, 25.62. Found: C, 14.16; H, 2.57; N, 3.31; Cl, 25.97. Selected IR (ν_{max}/cm^{-1}): 1607 m, 1417 s, 1124 and 1108.5 s, 1017 s, 806 s, 694 m, 512.0 w, 442 m, 428 m, 383 w, 344 m, 333 m. ^{1}H NMR (D_2O): δ 3.61 (s, 6H, $^3J_{PtH}$ = 25 Hz), −0.33 (br, 2H), −13.2 (br, 6H).

[$N(C_4H_9)_4$][$Ru^{III}Cl_4$(DMSO-S)(-μ-pyz)Pt^{II}(DMSO-S)Cl_2] (IT126). A 0.02 g portion of Na[*trans*-$RuCl_4$(DMSO)(pyz)] (0.06 mmol) was dissolved in 2 mL water and added to a stirring solution of 0.03 g K[$PtCl_3$(DMSO-S)] (0.06 mmol) in 2 mL water. The solution was stirred at room temperature for 1 h. At this point, 0.10 g (0.36 mmol) tetrabutylammonium chloride was dissolved in water and added to the stirring solution. The orange precipitate was formed immediately and collected by vacuum filtration, washed with diethyl ether, and vacuum-dried. A 0.030 g portion was obtained (54% yield). Selected IR (ν_{max}/cm^{-1}): 1608 m, 1425 m, 1124 s, 1025 s, 825 m, 680 m, 443 m, 423 m, 379 w, 346 m, 333 m. ^{1}H NMR (acetone-d_6): δ 3.01 (br, 8H), 2.76 (s, 6H, $^3J_{PtH}$ = 22 Hz), 1.25 (br, 8H), 0.82 (br, 8H), 0.35 (br, 12H), −0.01 (br, 2H), −11.8 (br, 6H). Suitable crystals were grown from acetone/ethanol. See the Supporting Information for crystallographic details, data table, and bond length/angle table.

Cell Motility Studies. Cell studies were conducted with the cell lines A549 and MDA-MB-231 (obtained from The American Type Culture Collection). Cells were grown in Click's RPMI growth medium supplemented with 10% FBS, nonessential amino acids, and antibiotics and kept at 37 °C, 5% CO_2.

A 24-well plate was treated with a collagen solution (500 mg/mL) and left at 4 °C overnight to settle. The collagen solution was aspirated and cells were seeded in the wells and allowed to grow to a confluent monolayer for 24 h (cells were seeded at 2.0×10^5 and 4.0×10^5 cells per well for A549 and MDA-MB-231 cells respectively). The wells were washed twice with serum-free medium prior to the formation of scratches. A single, vertical scratch was formed in the cell layer of each well using a p200 pipet tip of approximately 1 mm in diameter. The wells were then washed twice with serum-free medium, after which the medium was replaced with growth medium (1% FBS) containing the compounds, NAMI-A, AH197, IT127, or AH403 at varying concentrations.

Cells were visualized on an inverted microscope at a 10× objective, and pictures were taken with a Nikon digital camera immediately following initial treatment (t_0). Pictures were taken in the same locations after 24 h (t_{24}) of incubation at 37 °C in order to measure the ability of cells to fill in the artificial wound.

DNA Migration Studies. The plasmid pBluescript SK+ was purified from *E. coli* using a QIAGEN plasmid mini kit as described by the manufacturer (QIAGEN Inc.). Plasmid DNA was linearized with the restriction endonuclease *Eco*RI and purified from the reaction with a QIAquick PCR Purification Kit (QIAGEN Inc.) eluted in deionized water. The procedure used in these studies is a modification of that described by Stellwagen.[16] Briefly, 0.5 μg of linearized pBluescript SK+ was incubated with varying concentrations of the metal compounds in phosphate buffered saline (PBS; 3.8 mM NaH_2PO_4, 16.2 mM Na_2HPO_4, 150 mM NaCl, pH 6.4) in a total volume of 50 μL at 37 °C for 4 h. Following incubation, 20 μL samples were analyzed by agarose gel electrophoresis (0.9% agarose, 1X TBE (89 mM Tris base, 89 mM boric acid, 3.1 mM EDTA)). Gels were stained with 5 μg/mL ethidium bromide in 1X TBE for 45 min and photographed with UV illumination.

BSA Interaction Studies. All reactions of AH197, IT127, AH403, and NAMI-A with BSA were carried out in PBS (10 mM, pH 7.4).

Chart 1. Molecular Structures for the Compounds in This Study

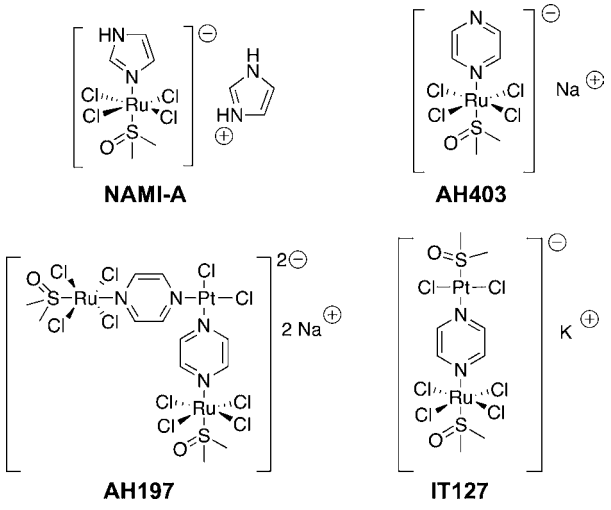

dx.doi.org/10.1021/ic301981s | Inorg. Chem. 2012, 51, 12917−12924

Reactions were monitored by UV/vis and absorption spectra were obtained at set time intervals with a compound to BSA ratio of 1:1 at a concentration of 50 μM. The compound and BSA solutions were mixed in a quartz cuvette immediately prior to the start of the study, and then, the reactions were monitored for 4 h, at 37 °C.

Additionally, AH197, IT127, and AH403 were tested as quenchers of the tryptophan residues in BSA. A 50 μM solution of BSA in PBS was treated with each of the quenchers in increments of 2 μL from a 10 mM stock solution, and the emission signal at 344 nm (excitation at 280 nm) was measured immediately following each addition.

RESULTS AND DISCUSSION

Synthesis and Characterization. The dinuclear species, K{[$Ru^{III}Cl_4$(DMSO-S)](μ-pyrazine)[Pt^{II}(DMSO-S)Cl_2]}, IT127, was synthesized from its ruthenium and platinum components (Scheme 1). It is very soluble in water, a desired property of cancer drugs as it eliminates the need for solubilizers in order to administer.

Scheme 1. Synthesis of Dinuclear Species

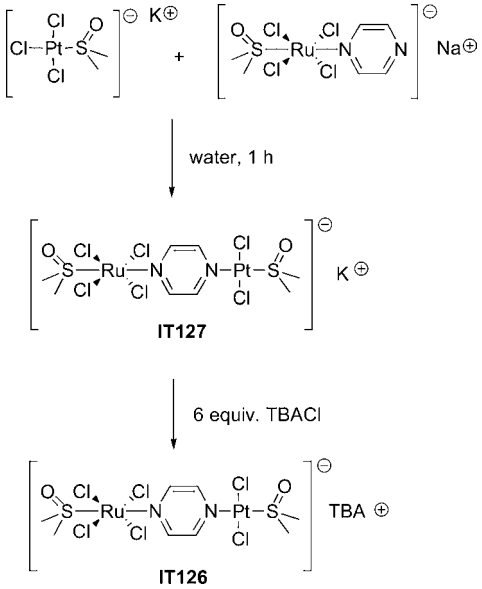

The tetrabutylammonium (TBA) dinuclear species, TBA-{[$Ru^{III}Cl_4$(DMSO-S)](μ-pyrazine) [Pt^{II}(DMSO-S)Cl_2]}, IT126, was synthesized by adding an excess of TBA to an aqueous solution of IT127, and its structure determined by XRD, in order to confirm the structure of the complex anion, as suitable crystals of IT127 could not be grown. The molecular structure of IT126 was determined to have trans stereochemistry at both the platinum and ruthenium metal centers (Figure 1). Bond lengths are in the acceptable range with comparable complexes (AH197 and AH229).[9a] The Pt−N(2) bond is slightly longer in IT127 which can be attributed to the pyrazine being trans to the dmso ligand in IT127, which has greater pi acidity than the chloride ligand in AH197. The trans species is expected to form immediately, as dmso has a greater trans effect than chloride,[17a] and remain inert to isomerization, as trans monomeric and trans−trans dimeric platinum compounds with pyrazine and sulfoxide ligands are known not to isomerize to the corresponding cis species.[17] In addition, in the case of AH197, due to the choice of the cis starting material, cis-[$PtCl_2$(pyrazine)$_2$], the initially formed cis species isomerizes to the trans species, over a period of several hours to days (depending on the conditions) indicating that the trans species is more stable than the cis.[9a] Despite the paramagnetic ruthenium(III) center, IT127 was partially characterized by NMR spectroscopy. One peak corresponding to the Ru-dmso methyl protons is observed upfield as a very broad band at approximately −13.2 ppm. The pyrazine protons ortho to the platinum are observed at −0.45 ppm, while the ring protons ortho to the paramagnetic ruthenium are too broad to be observed. This is similar to other paramagnetic ruthenium(III) complexes previously reported.[9,14a] A second dmso peak is observed for the Pt-dmso ligand at 3.61 ppm having platinum satellites of 25 Hz. Furthermore, addition of the reducing agent ascorbic acid immediately reduced the ruthenium(III) to ruthenium(II), with the upfield peaks, associated with the paramagnetic center, disappearing and several others in the regular diamagnetic region of the spectrum appearing. As a number of peaks are observed, it can be speculated that a mixture of hydrolysis species had formed once the ruthenium had been reduced.[9,14a]

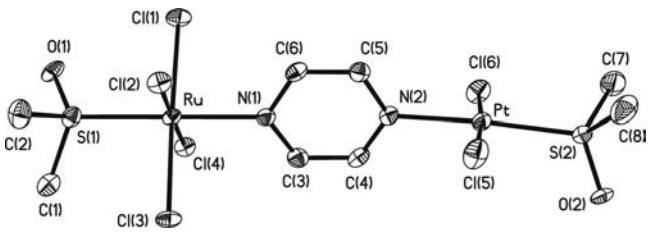

Figure 1. Molecular structure of the IT126 dinuclear anion.

Cell Motility Studies. Four metal complexes were tested for their ability to inhibit cell motility in the A549 (nonsmall cell lung) and MDA-MB-231 (breast) cancer cell lines. As both cell lines are highly invasive and have been used for similar motility assays in previous studies, they were deemed especially suitable for use in the evaluation of the Ru^{III}−Pt^{II} compounds presented in this study as antimetastatic agents.[18] Cell motility studies were conducted with the A549 cells, yielding promising results for AH197 in comparison to NAMI-A as a motility inhibitor. The studies were continued with MDA-MB-231 cells, as the NCI-60 screening for AH197 showed good antiproliferative potential against this particular cell line in comparison to cisplatin (IC50 ratio of AH197/cisplatin = 0.51).[9a]

Both cell systems were initially allowed to reach confluence within 24 h, forming a uniform monolayer of cells on the well-plate. A single vertical scratch, or wound, was made in each well with a pipet tip of approximately 1 mm in width (Figure 2). The growth medium was then replaced with new medium that contained solutions of the metal complexes, AH197, IT127, a mononuclear Ru^{III} compound, AH403, and the ruthenium, anticancer agent, NAMI-A. Cell movement across the gaps/wounds was observed 24 h post-treatment under an objective of 10×. In the absence of any compound, the gaps were completely closed after 24 h. However, 100 μM treatments showed a clear divergence in cell migratory behavior in both cell lines, where the inhibitory effect was as follows: AH197 > IT127 > NAMI-A > AH403 (Figure 2). The effect was clearly shown to be greater for the trinuclear species than NAMI-A, the ruthenium drug which is a seminal entry in the next generation of anticancer metal chemotherapeutics. It appears that as the number of metal centers increases in the complex, most importantly ruthenium centers, the greater the inhibition of cell motility. Furthermore, of the four compounds studied, AH197 showed the strongest inhibition of cell movement at

dx.doi.org/10.1021/ic301981s | Inorg. Chem. 2012, 51, 12917−12924

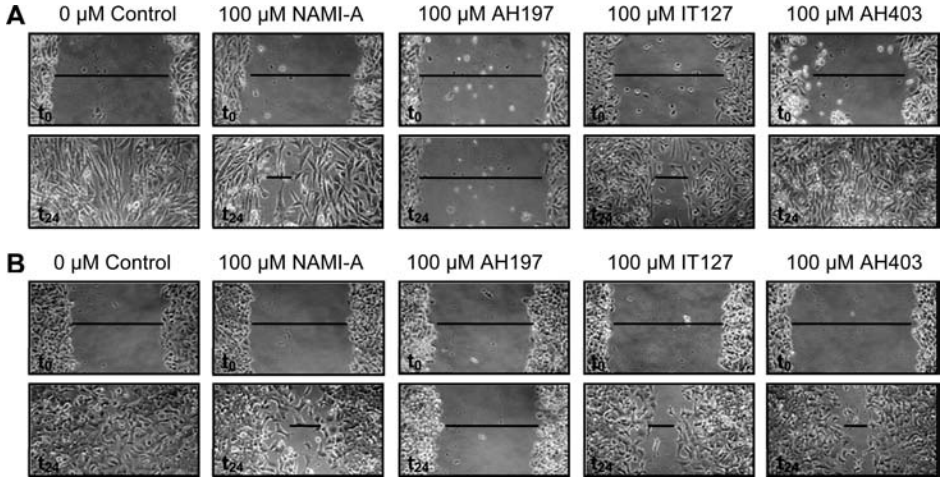

Figure 2. Cell motility studies with NAMI-A, AH197, IT127, and AH403 at 100 μM and a 0 μM control with the (A) MDA-MB-231 and (B) A549 cell lines. Images were taken in identical locations at 0 and 24 h. Scratch size varies but is approximately 1 mm in width at t_0.

concentrations below 100 μM on MDA-MB-231 cells. Complete inhibition was observed at 10 μM, while at 1 μM, the level of inhibition was comparable to that of NAMI-A at 100 μM, suggesting that AH197 exerts an inhibitory effect that is approximately 2 orders of magnitude greater than that of NAMI-A (see Figures 2SI and 3SI in the Supporting Information). However, in the A549 cell line, AH197 appears to exert an inhibitory effect of approximately 1 order of magnitude greater than NAMI-A. This is promising, as, although the antimetastatic properties of ruthenium complexes are not completely understood, inhibition of cell motility has been reported to be related to the antimetastatic nature of the complexes.[6]

DNA Gel Electrophoresis. The ability of cisplatin to cause helical distortion in DNA has been widely accepted as the drug's primary mode of action in its attack on cancer cells.[2c] The platinum center is known to form intrastrand cross-links with guanine bases that bend DNA.[2f] This can be observed by a marked reduction in the electrophoretic mobility of DNA upon the introduction of cisplatin.[2f] The concentration dependent inhibition of DNA migration due to incubation with AH197 was shown to have a greater effect than cisplatin, suggesting it also tightly binds to DNA.[9a] Figure 3 shows the comparison of electrophoretic mobility inhibition for cisplatin, AH197, and the new binuclear species, IT127. Interestingly, IT127 appears to have a greater effect on mobility than cisplatin and AH197 at comparable concentrations (Figure 3; lanes 3–5 with lanes 8–10) with the order of inhibition being IT127 > AH197 > cisplatin (Figure 3).

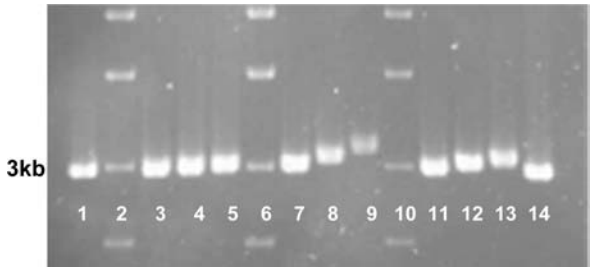

Figure 3. Gel electrophoresis of cisplatin, AH197, and IT127. Linearized plasmid DNA was incubated with compounds at varying concentrations for 4 h at 37 °C. Lanes 2, 6, 10: 1 kb ladder. Lanes 1 and 14: 0 mM control DNA. Lanes 3–5: cisplatin at 0.1, 0.5, and 1.0 mM. Lanes 7–9: IT127 at 0.1, 0.5, and 1.0 mM. Lanes 11–13: AH197 at 0.1, 0.5, and 1.0 mM.

In this experiment, concerned with the interaction of metal complexes with DNA, the dinuclear compound IT127 has a much greater effect than either AH197 or cisplatin (the standard for metal chemotherapeutics), and this may be attributed to its size, nuclearity, and geometry. Given the results (Figure 3), IT127 is expected to make different linkages to DNA, whether intra or interstrand, causing large distortion of the DNA molecule. Similar mononuclear ruthenium complexes have been reported to have little effect on electrophoretic mobility and thus small initial interactions are expected for ruthenium centers. However, one could speculate that once the platinum has made its initial bond to a DNA base, the ruthenium might be well-positioned to make covalent interactions with other bases in close proximity, whether inter or intrastrand, thus subsequently causing greater distortion of the molecule and greater inhibition of mobility. Simple ruthenium(III)/DMSO compounds are hypothesized to act on tumor cells through mechanisms different from that of cisplatin, not necessarily involving interactions with DNA.[4a] These results indicate that our hybrid complexes containing both ruthenium and platinum may be effective in many ways involving both DNA and other biomolecules, as the extent of the effect on cell motility is reversed compared to the effect on DNA migration.

NCI's 60 Cell Line in vitro Screening. IT127 was submitted to NCI's Developmental Therapeutics Program for testing. A single dose analysis of the compound was performed against the 60 Human Tumor cell lines used by this program for in vitro screening. On the basis of the activity of a compound against the 60 cell lines, the COMPARE[19] algorithm, developed at the NCI, calculates Pearson correlation coefficients for compounds, against all other compounds in the database (standard COMPARE), or against any subset of compounds within the database defined by the user (matrix COMPARE).

A matrix COMPARE was performed with AH197, IT127, cisplatin, and a ruthenium(III) drug currently in clinical trials, KP1019[5d] (Table 1). While AH197 is not significantly correlated with IT127, cisplatin, or KP1019, IT127 is correlated with cisplatin, and with KP1019. It is particularly interesting,

Table 1. Pearson Correlation Coefficient from the Matrix COMPARE Algorithm

	AH197	IT127	cisplatin
IT127	−0.17		
cisplatin	0.19	0.36[b]	
[c]KP1019	0.25	0.28[a]	0.18

[a]$p < .05$. [b]$p < .005$. [c]Only data for 100 μM KP1019 is available in the NCI database.

given the effect of increased numbers of ruthenium centers on cell motility (Figure 2), that a reduction in ruthenium centers makes the compounds more KP1019-like in terms of their effects on cell proliferation. It appears added ruthenium centers enhance both the antimetastatic activities of the compounds, as seen in Figure 2, and fundamentally alter their interactions with targets involved in cell proliferation or survival (Table 1). The influence of ruthenium centers on heteronuclear compounds is highlighted by the differences in correlation coefficients of AH197 and IT127 when compared to cisplatin (Table 1). While it is tempting to suggest that ruthenium centers may inhibit the ability of the heteronuclear complexes to interact with DNA, the mobility shift assay (Figure 3) suggests that ruthenium centers enhance either binding affinities or the structural impact of binding on DNA. Therefore, it is uncertain whether the differences in their impacts on cell growth and survival are mediated by interactions with proteins or interactions with other cellular components rather than compound/DNA interactions.

Since high Pearson correlation values are indicative of similar mechanisms of action, we performed a standard COMPARE analysis against IT127 and AH197 (Table 2). As seen in the matrix COMPARE in Table 1, IT127 correlates significantly with cisplatin and AH197 does not. AH197 and IT127 correlate with five drugs in common. IT127 was not considered for further evaluation by the NCI after the single dose analysis had been performed. However, it has been suggested that this screening procedure is not necessarily the most appropriate for the full assessment of both antineoplastic and antimetastatic drugs.[4d]

Table 2. Selected Results of Standard COMPARE Analyses of AH197 and IT127[a]

	AH197	IT127
cisplatin		0.36 (3)
caracemide	0.37 (2)	0.31 (7)
pibenzimol hydrochloride	0.40 (0)	0.27 (2)
flavoneacetic acid	0.38 (4)	0.31 (6)
cyclopentenylcytosine	0.41 (3)	0.27 (2)
DON	0.43 (2)	0.36 (2)

[a]Compounds with Pearson correlation significance ($p < .05$) for both AH197 and IT127 are shown. Numbers in parentheses are the absolute rank among all compounds in the database against the compound heading the column. e.g. One means that compound showed the strongest correlation.

X-ray Absorption Spectroscopy, UV/vis Spectroscopy, and Emission Spectroscopy. Several of the complexes, along with their adducts with bovine serum albumin (BSA), were studied using X-ray absorption spectroscopy (XAS). This technique has been employed recently in order to probe the oxidation state of the ruthenium species and to determine if substitution reactions have occurred at the metal center.[6a,12] Spectra were run under several different conditions before and after adduct formation in order to aid in characterization of the metal/protein adducts. The metal complexes AH197, IT127, AH403, and NAMI-A all showed spectra similar to those recently reported for Ru^{III}-/chloro/dmso complexes, featuring well-defined shoulders on the lower energy side of the Ru L_3-edge and Cl K-edge peaks (Figure 4).[6a,12] Adduct samples were prepared by incubation of the compounds with BSA in phosphate buffer (PB) at 37 °C for 4 h. The spectra of these adducts showed an almost complete reduction of the Cl K-edge peak, along with a loss of the definition of the shoulder on the Ru L_3-edge peak (Figure 4). This led us to conclude that the chloride ligands had been substituted by electron-donating residues in the protein, most likely nitrogen or sulfur donating groups, as has been suggested in previous studies of interactions between ruthenium complexes and BSA.[12b] Similar results were obtained when adducts were prepared by incubation of the compounds and protein for 24 h.

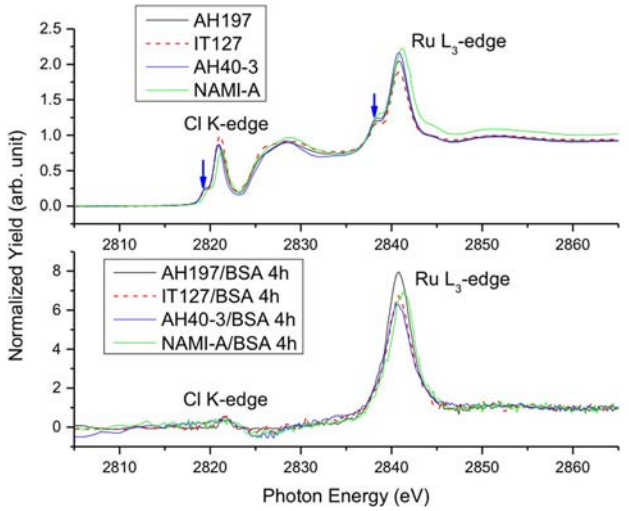

Figure 4. XAS of metal complexes (NAMI-A, AH197, IT127, and AH403) as controls (top) and of samples incubated with BSA for 4 h at 37 °C in PB (bottom).

When phosphate buffered saline (PBS) was used, instead of the nonsaline PB buffer, under similar conditions, the Cl K-edge peak was still present to a significant degree, indicating that the higher concentration of chloride in the PBS buffer solution must inhibit the dissociation of all of the chloride ligands (Figure 6). Once again, the shoulder characteristic of ruthenium(III) has lost its definition to a considerable degree. This loss of definition could be the result of reduction of a portion of the ruthenium(III) metal centers to ruthenium(II) and thus a mixture of species with different oxidation states is observed. Another possibility is that the substitution of donors from the protein and/or water molecules for the chloride ligands to form the adduct samples has sufficiently lowered the symmetry causing a broadening of the peaks and thus a loss of the fine structure that had been observed in the original metal samples. The intensity of the Ru L_3 peak is reduced considerably from the pure sample compared to the adducts, most likely due to adduct formation. The large amount of protein present in the adduct reduces the relative amount of free ruthenium in the sample or the effective concentration of ruthenium in the beam. The Cl K-edge peak was clearly

dx.doi.org/10.1021/ic301981s | Inorg. Chem. 2012, 51, 12917−12924

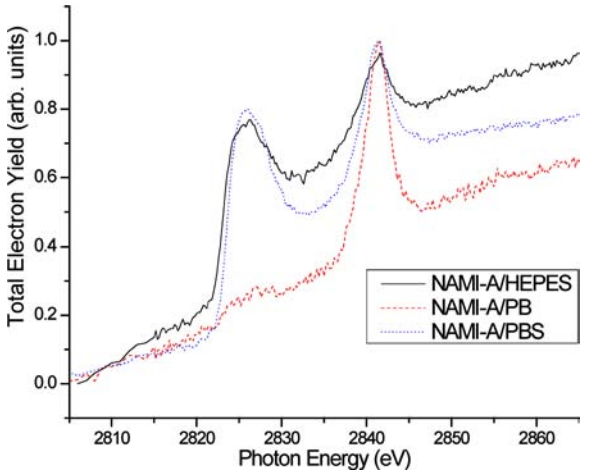

Figure 5. XAS spectra of NAMI-A incubated with BSA at 37 °C for 4 h in three different buffer systems: PBS, HEPES, and PB.

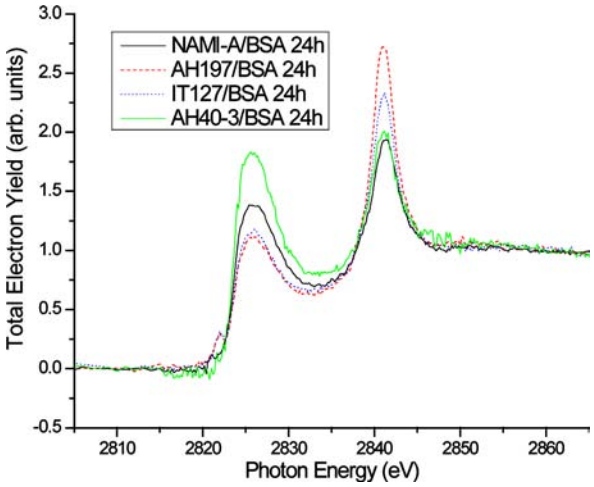

Figure 6. XAS spectra of the ruthenium-containing complexes incubated with BSA for 24 h at 37 °C in PBS.

present, in NAMI-A adducts, when the HEPES buffer conditions described by Liu et al. were followed and when PBS was used, however, the peak is virtually absent when the buffer PB was used (Figure 5).[6a] This is consistent with our results in that the HEPES buffer contains a chloride concentration similar to that of PBS. In addition, we cannot state, as reported,[12b] that the ruthenium unambiguously remains in the +3 oxidation state. In that report, PB was reported as the buffer system and no chloride concentration was mentioned. It appears that there is a considerable retardation of chloride dissociation in saline systems compared to nonsaline buffer conditions, which would be reasonable. Chloride dissociation slowed considerably as the concentration of chloride was increased in similar ruthenium systems.[10d] Given the spectroscopic results above, we suggest that chloride substitution occurs quickly in both PB and PBS; however, the substitution is complete within 4 h in PB but is slowed down due to the increased saline concentration in PBS. Therefore, chloride peaks are still evident in that system as shown by XAS even after several hours of incubation.

In an attempt to further elucidate the nature of the substitution reactions occurring, UV/vis spectra were run monitoring the reactions of AH197 and IT127 with the BSA. In these cases, reactions were done separately in PBS and PB and similar results were obtained (see SI for plots). In all cases the MLCT peak at around 400 nm reduces quickly as the reaction proceeds. In the case of AH197 (Figure 4SI), a new peak grows at around 475 nm and a very low intensity peak at 550 nm appears. On the other hand, new peaks at lower energy were not observed to form for the reactions of NAMI-A, IT127, or AH403 with BSA. The isolation of metal−protein adducts by various drying techniques yielded deep purple solids, a clear visible change from the original yellow/orange solutions. However, the spectral pattern of change, with respect to time, as the reaction occurs with protein is not very different from that of the metal complexes in aqueous solution, when no protein is present and hydrolysis is known to occur.[9a] The UV/vis spectra definitely indicate substitution reactions; however, the spectra give little insight into which ligands/donors have replaced the chlorides after their initial dissociation. It appears that XAS is a better probe into this reaction, usually probed using UV/vis spectroscopy and that XAS may deserve more attention in the future.

As further evidence of the interaction between the complexes and BSA, a simple quenching experiment was carried out. The intensity of emission by the two tryptophan residues (134 and 212) of the protein was measured as a result of adding the compounds, AH197 and IT127. The complexes act as quenchers, by interacting with tryptophan or other N-/S-donating residues, altering the secondary structure of the protein, thus reducing the intensity of emission by tryptophan.[20] Both AH197 and IT127 succeeded as quenchers of the emission signal at 344 nm; however, it took

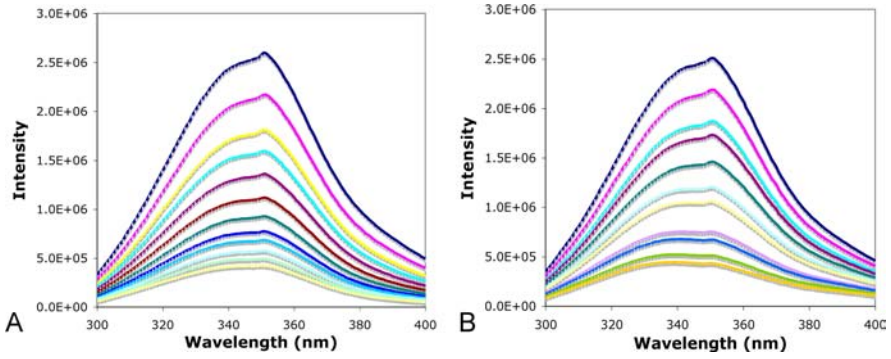

Figure 7. Quenching of tryptophan emission in BSA with (A) successive additions of AH197 to 1.5 equiv total and (B) successive additions of IT127 to 3.0 equiv total. Intensity of emission decreases with addition of complexes.

approximately half the number of equivalents of AH197 to quench the signal as it did for IT127. Figure 7 shows the decrease in intensity as the compounds were added to a solution of BSA in PBS buffer. It is suspected that the difference in quenching capacity between these two compounds could be a reflection, once again, of the number of ruthenium centers present, where AH197, the trinuclear Ru_2Pt species, appears to be superior. However, this could also be a result of other factors such as size or geometry.

CONCLUDING REMARKS

A new dinuclear platinum/ruthenium complex was synthesized and characterized. It, along with the already reported trinuclear species, AH197, and the known anticancer agents NAMI-A and cisplatin were subjected to a variety of experiments to determine their reactivity with relevant biomolecules and cancer cells. The structures of the metal/protein adducts were probed using XAS. General ideas about the binding of the metal centers to BSA, about ligand substitution, and about oxidation state of the metal were gained. XAS has been shown to be a valuable probe for metal/protein interactions. The hetero-multinuclear complexes exhibited greater degrees of interaction with DNA and greater inhibition of cell motility, two important properties in assessing the potency of new metallic drugs, than the well-known metal chemotherapeutics, cisplatin, and NAMI-A. This leads us to conclude that our multinuclear hybrids show promise as anticancer agents exhibiting a wide range of activity with biomolecules thought to be important in the assessment of their efficacy. Our results support the notion of a synergistic effect between the two metal-centered systems. Future studies are in progress with the aim of exploring the effect of nuclearity on reactivity.

ASSOCIATED CONTENT

Supporting Information

Further experimental details, crystallographic details and tables, cell motility figures as a function of concentration for all compounds, UV/vis spectra of the reaction of metal complexes with BSA, and CIF for compound IT126. This material is available free of charge via the Internet at http://pubs.acs.org.

AUTHOR INFORMATION

Corresponding Author

*E-mail: canderso@bard.edu. Phone: 845-752-2356. Fax: 845-752- 2339.

Notes

The authors declare no competing financial interest.

ACKNOWLEDGMENTS

We would like to thank the support of The Camille and Henry Dreyfus Foundation by granting Craig M. Anderson a Henry Dreyfus Teacher-Scholar Award. This work is also supported by the NSF (CHE-1058936, C.M.A., PI). The authors also thank Bard College and BSRI for additional support. We thank Prof. Christopher LaFratta and Ian Pelse for help with the atomic emission spectroscopy. The XAS measurement was performed using the SXRMB beamline at the Canadian Light Source, which is financially supported by NSERC, NRC, CIHR, and University of Saskatchewan.

REFERENCES

(1) (a) Chabner, B. A.; Roberts, T. G. *Nat. Rev. Cancer* **2005**, *5*, 65–72. (b) Bernier, J.; Hall, E. J.; Giaccia, A. *Nat. Rev. Cancer* **2004**, *4*, 737–747.

(2) (a) Clarke, M. J. *Coord. Chem. Rev.* **2003**, *236*, 209–233. (b) Fuertes, M. A.; Alonso, C.; Perez, J. M. *Chem. Rev.* **2003**, *103*, 645–662. (c) Zhang, C. X.; Lippard, S. J. *Curr. Opin. Chem. Bio.* **2003**, *7*, 481–489. (d) Thayer, A. *C&E News* **2010**, *88*, 24–28. (e) Klein, A. V.; Hambley, T. W. *Chem. Rev.* **2009**, *109*, 4911–4920. (f) Jamieson, E. R.; Lippard, S. J. *Chem. Rev.* **1999**, *99*, 2467–2498.

(3) Price, J. T.; Thompson, E. W. *Expert Opin. Ther. Targets* **2002**, *6*, 217–233.

(4) (a) Casini, A.; Hartinger, C. G.; Nazarov, A. A.; Dyson, P. J. *Top. Organomet. Chem.* **2010**, *32*, 57–80. (b) Kostova, I. *Curr. Med. Chem.* **2006**, *13*, 1085–1107. (c) Antonarakis, E.; Emadi, A. *Cancer Chemother. Pharmacol.* **2010**, *66*, 1–9. (e) Alessio, E. *Chem. Rev.* **2004**, *104*, 4203–4242. (d) Dyson, P. J.; Sava, G. *Dalton Trans.* **2006**, 1929–1933.

(5) (a) Alessio, E.; Mestroni, G.; Bergamo, A.; Sava, G. *Curr. Top. Med. Chem.* **2004**, *4*, 1525–1535. (b) Auzias, M.; Gueniat, J.; Therrien, B.; Suss-Fink, G.; Renfrew, A. K.; Dyson, P. J. *J. Orgomet. Chem.* **2009**, *694*, 855–861. (c) Pizarro, A. M.; Habtemariam, A.; Sadler, P. J. *Top. Organomet. Chem.* **2010**, *32*, 21–56. (d) Hartinger, C. G.; Jakupec, M. A.; Zorbas-Seifried, S.; Groessl, M.; Egger, A.; Berger, W.; Zorbas, H.; Dyson, P. J.; Keppler, B. K. *Chem. Biodivers.* **2008**, *10*, 2140–55.

(6) (a) Liu, M.; Lim, Z. J.; Gwee, Y. Y.; Levina, A.; Lay, P. A. *Angew. Chem., Int. Ed.* **2010**, *49*, 1661–1664. (b) Messori, L.; Vilchez, F. G.; Vilaplana, R.; Piccioli, F.; Alessio, E.; Keppler, B. *Met. Based Drugs.* **2000**, *7* (6), 335–42.

(7) (a) Davies, M. S.; Thomas, D. S.; Hegmans, A.; Berners-Price, S. J.; Farrell, N. *Inorg. Chem.* **2002**, *41*, 1101–1109. (b) Komeda, S.; Moulaei, T.; Woods, K. K.; Chikuma, M.; Farrell, N. P.; Williams, L. D. *J. Am. Chem. Soc.* **2006**, *48*, 7413–7420. (c) Hegmans, A.; Berners-Price, S. J.; Davies, M. S.; Thomas, D. S.; Humphreys, A. S.; Farrell, N. *J. Am. Chem. Soc.* **2004**, *126*, 2166–2180. (d) Harris, A. L.; Qu, Y.; Farrell, N. P. *Inorg. Chem.* **2005**, *44*, 1196–1198. (e) Harris, A. L.; Yang, X.; Hegmans, A.; Povirk, L.; Ryan, J. J.; Kelland, L.; Farrell, N. P. *Inorg. Chem.* **2005**, *44*, 9598–9600.

(8) (a) Higgins, S.; White, T.; Winkel, B.; Brewer, K. J. *Inorg. Chem.* **2011**, *50*, 463–470. (b) Higgins, S.; Tucker, A.; Winkel, B.; Brewer, K. J. *Chem. Commun.* **2012**, *48*, 67–69.

(9) (a) Herman, A.; Tanski, J. M.; Tibbetts, M. F.; Anderson, C. M. *Inorg. Chem.* **2008**, *47*, 274–280. (b) Anderson, C. M.; Herman, A.; Rochon, F. *Polyhedron* **2007**, *26*, 3661–3668.

(10) (a) Anderson, C.; Beauchamp, A. L. *Inorg. Chem.* **1995**, *34*, 6065–6073. (b) Anderson, C. *Can. J. Chem.* **2001**, *79*, 1477–1482. (c) Anderson, C.; Beauchamp, A. L. *Inorg. Chim. Acta* **1995**, *233*, 33–41. (d) Anderson, C.; Beauchamp, A. M. *Can. J. Chem.* **1995**, *34*, 6065–6073.

(11) (a) Webb, M. I.; Chard, R. A.; Al-Jobory, J. M.; Jones, M. R.; Wong, E.; Walsby, C. J. *Inorg. Chem.* **2012**, *51*, 954–966. (b) Webb, M. I.; Walsby, C. J. *Dalton Trans.* **2011**, *40*, 1322.

(12) (a) Harris, T. V.; Szilagyi, R. K.; McFarlane Holman, K. L. *J. Bio. Inorg. Chem.* **2009**, *14*, 891–898. (b) Ascone, I.; Messori, L.; Casini, A.; Gabbiani, C.; Balerna, A.; Dell'Unto, F.; Castellano, A. *Inorg. Chem.* **2008**, *47*, 8629–8634.

(13) Messori, L.; Orioli, P.; Vullo, D.; Alessio, E.; Iengo, E. *Eur. J. Biochem.* **2000**, *267*, 1206–1213.

(14) (a) Iengo, E.; Mestroni, G.; Geremia, S.; Calligaris, M.; Alessio, E. *Dalton Trans.* **1999**, *4*, 3361–3371. (b) Kukushkin, Y. N.; Vyazmenski, Y. E.; Zorina, L. I. *Russ. J. Inorg. Chem.* **1968**, *13*, 1573. (c) Mestroni, G.; Alessio, E.; Sava, G. *New salts of anionic complexes of Ru(III), as antimetastatic and antineoplastic agents*. World Intellectual Property Organization, International Bureau, 1998, WO 98/00431.

(15) LaFratta, C.; Jain, S.; Pelse, I.; Simoska, O.; Elvy, K. *J. Chem. Educ.* **2012**, accepted for publication.

(16) Stellwagen, N. *Nucleic Acid Electrophoresis*; Springer: Berlin, 1998; pp 1–53.

(17) (a) Kukushkin, V. Y.; Pombeira, A. J. L.; Ferreira, C. M. P.; Elding, L. I. *Inorg. Synth.* **2002**, *33*, 189−196. (b) Rochon, F. D.; Priqueler, J. R. L. *Can. J. Chem.* **2004**, *82*, 649−658. (c) Priqueler, J. R. L.; Rochon, F. D. *Inorg. Chim. Acta* **2004**, *357*, 2167−2175.
(18) (a) Hulkower, K. I.; Herber, R. L. *Phramacuetics* **2011**, *3*, 107−124. (b) Pellegrino, T.; Parak, W. J.; Boudreau, R.; Le Gros, M. A.; Gerion, D.; Alivisatos, A. P.; Larabell, C. A. *Differentiation* **2003**, *71*, 542−548. (c) Chang, C.; Shih, J.; Jeng, Y.; Su, J.; Lin, B.; Chen, S.; Chau, Y.; Yang, P.; Kuo, M. *J. Natl. Cancer. Inst.* **2004**, *5*, 364−375.
(19) (a) Boyd, M. R.; Paull, K. D. *Drug. Dev. Res.* **1995**, *34*, 91−109. (b) Holbeck, S. L.; Collins, J. M.; Doroshow, J. H. *Mol. Cancer Ther.* **2010**, *5*, 1451−1460.
(20) Bhat, S. S.; Kumbhar, A. A.; Heptullah, H.; Khan, A. A.; Gobre, V. V.; Gejji, S. P.; Puranik, V. G. *Inorg. Chem.* **2011**, *50*, 545−558.